

Kinetic Properties of *ba*₃ Oxidase from *Thermus thermophilus*: Effect of Temperature[†]

Alessandro Giuffrè,[‡] Elena Forte,[‡] Giovanni Antonini,^{‡,§} Emilio D'Itri,[‡] Maurizio Brunori,^{*,‡}
Tewfik Soulimane,^{||} and Gerhard Buse^{||}

Department of Biochemical Sciences and CNR Center of Molecular Biology, University of Rome "La Sapienza", Rome, Italy,
Department of Basic and Applied Biology, University of L'Aquila, L'Aquila, Italy, and Institut für Biochemie,
Rheinisch-Westfälische Technische Hochschule, Aachen, Germany

Received June 29, 1998; Revised Manuscript Received October 5, 1998

ABSTRACT: The kinetic properties of the *ba*₃ oxidase from *Thermus thermophilus* were investigated by stopped-flow spectroscopy in the temperature range of 5–70 °C. Peculiar behavior in the reaction with physiological substrates and classical ligands (CO and CN[−]) was observed. In the O₂ reaction, the decay of the F intermediate is significantly slower (*k*' = 100 s^{−1} at 5 °C) than in the mitochondrial enzyme, with an activation energy *E*^{*} of 10.1 ± 0.9 kcal mol^{−1}. The cyanide-inhibited *ba*₃ oxidizes cyt *c*₅₅₂ quickly (*k* ≈ 5 × 10⁶ M^{−1} s^{−1} at 25 °C) and selectively, with an activation energy *E*^{*} of 10.9 ± 0.9 kcal mol^{−1}, but slowly oxidizes ruthenium hexamine, a fast electron donor for the mitochondrial enzyme. Cyt *c*₅₅₂ oxidase activity is enhanced up to 60 °C and is maximal at extremely low ionic strengths, excluding formation of a high-affinity cyt *c*₅₅₂–*ba*₃ electrostatic complex. The thermophilic oxidase is less sensitive to cyanide inhibition, although cyanide binding under turnover is much quicker (seconds) than in the fully oxidized state (days). Finally, the affinity of reduced *ba*₃ for CO at 20 °C (*K*_{eq} = 1 × 10⁵ M^{−1}) was found to be smaller than that of beef heart *aa*₃ (*K*_{eq} = 4 × 10⁶ M^{−1}), partly because of an unusually fast, strongly temperature-dependent CO dissociation from cyt *a*₃²⁺ of *ba*₃ (*k*' = 0.8 s^{−1} vs *k*' = 0.02 s^{−1} for beef heart *aa*₃ at 20 °C). The relevance of these results to adaptation of respiratory activity to high temperatures and low environmental O₂ tensions is discussed.

The *ba*₃ cytochrome *c* oxidase of *Thermus thermophilus* HB8 (ATCC 27634) is one of the two terminal oxidases expressed by this thermophilic, Gram-negative eubacterium. This enzyme, although belonging to the heme–copper oxidase superfamily, shows several peculiar properties. First isolated by Zimmermann et al. (1), its amino acid sequence (2) revealed very low homology (<20% identities) with most terminal oxidases, and it was suggested to belong to the *Sox-B* cluster (3, 4) together with other phylogenetically distant oxidases already partly characterized [such as *Sox-ABCD* of *Sulfolobus acidocaldarius* (5–7) and *aa*₃ of *Acidianus ambivalens* (8–10)]. Our interest in the *ba*₃ oxidase is justified by the fact that the X-ray structure of this enzyme is being investigated (11) and may soon be available, and the three-dimensional structure of its physiological substrate, cytochrome *c*₅₅₂, has been solved (12, 13), revealing unique features which may account for the high thermostability (14) and the highly selective interaction with its oxidase (12).

By several different techniques [FT-IR¹ (15), RR and EPR (16, 17), and CD and MCD (18) both static or combined with flash photolysis], prior studies clearly showed that the cyt *a*₃–Cu_B of *ba*₃ has peculiar ligand binding properties, leading to the conclusion that this site will reveal significant structural differences as compared with other members of the heme–copper oxidase superfamily (19–22). Remarkable differences were found in the binding of carbon monoxide (CO) to the reduced cyt *a*₃–Cu_B site: an unusually high IR frequency of the Fe–CO complex (15), a much higher affinity of Cu_B⁺ for CO (*K* > 10⁴ M^{−1}), and a much slower intramolecular ligand transfer to cyt *a*₃²⁺ (*k* = 8 s^{−1}) as compared to those of the mitochondrial enzyme (23). In particular, an IR study with the *ba*₃–CO complex (15) showed that under photostationary illumination CO is quantitatively transferred to Cu_B⁺ even at room temperature, whereas in beef heart oxidase after photodissociation, the lifetime of the Cu_B⁺–CO complex is only 1.5 μs (24). These studies suggest an unusually low affinity of CO for ferrous cyt *a*₃ in the bacterial enzyme and demand a more complete kinetic investigation extended to physiological temperatures. Likewise, cyanide binding to oxidized *ba*₃ (16, 17) demands hours to days (depending on the age of the enzyme) and yields a one-electron reduced adduct with reduced cyt *a*₃ and two molecules of CN[−] bound.

[†] A.G. was supported by a fellowship from Centro Interdisciplinare Linceo of the "Accademia Nazionale dei Lincei" of Italy. The work was partially supported by MURST of Italy (Progetti Nazionali di Ricerca, ex-40%) and by the Deutsche Forschungsgemeinschaft to G.B. (Bu 463, 3-2).

^{*} To whom correspondence should be addressed: Dipartimento di Scienze Biochimiche "A. Rossi-Fanelli", Università di Roma "La Sapienza", P.le Aldo Moro 5, I-00185 Rome, Italy. Telephone: 39-6-4450291. Fax: 39-6-4440062. E-mail: brunori@axrma.uniroma1.it.

[‡] University of Rome "La Sapienza".

[§] University of L'Aquila.

^{||} Rheinisch-Westfälische Technische Hochschule.

¹ Abbreviations: RR, resonance Raman; CD, circular dichroism; MCD, magnetic circular dichroism; EPR, electron paramagnetic resonance; FT-IR, Fourier transform infrared spectroscopy; SVD, singular value decomposition; cyt, cytochrome; eT, electron transfer.

In this paper, we explore with stopped-flow techniques and over a wide temperature range (5–70 °C) the kinetic behavior of *ba*₃ in the reaction with substrates (cyt *c*₅₅₂ and O₂) and ligands (CO and CN[−]). The O₂ reaction was found to be remarkably sensitive to temperature, being below 30 °C unusually slow for a terminal oxidase; we postulate that this atypical kinetic behavior may provide an explanation for the thermophilicity of *ba*₃. The reaction with cyt *c*₅₅₂ was found to be fast, selective, and, interestingly, maximal at very low ionic strengths, suggesting no formation of a high-affinity complex with *ba*₃, contrary to horse heart cyt *c* with bovine and *Paracoccus denitrificans* oxidases (25–27). Finally, we demonstrate that in the *ba*₃ oxidase the low CO affinity displayed by cyt *a*₃²⁺ (i) is due to an unusually fast thermal dissociation of the ligand and (ii) is partly compensated by an atypical large CO affinity of Cu_B⁺. From this peculiar behavior, we infer that in thermophilic oxidases Cu_B⁺ may act as an efficient “trap” for O₂, present only at low concentrations in the physiological environment due to the reduced gas solubility at high temperatures.

MATERIALS AND METHODS

Materials. Ascorbate, tetramethyl-*p*-phenylenediamine (TMPD), and ruthenium(III) hexamine were from Sigma (St. Louis, MO). Dodecyl β-D-maltoside was from Biomol (Hamburg, Germany). Stock solutions of CO or NO (Air Liquide, Paris, France) were prepared by equilibrating degassed buffer with the pure gases ([NO] = 2 mM and [CO] = 1 mM in solution at 20 °C). All the experiments were performed in 0.1 M Tris (pH 7.6) and 0.05% lauryl maltoside (unless otherwise specified). Cyanide-inhibited *ba*₃ was prepared by incubating the enzyme for 5 days at 45 °C with 3 mM NaCN.

Enzyme Purification. Fermentation of *T. thermophilus* HB8 (ATCC 27634) has been performed at the Gesellschaft für Biotechnologische Forschung (GBF) Braunschweig. For the expression of the cytochrome *c*₅₅₂ and *ba*₃ oxidase, the cells were grown at 70 °C in 100 L of culture medium using a stainless steel jar fermenter under 0.05 V V^{−1} min^{−1} (volume of air per volume of medium per minute). The cells were harvested in the early to middle exponential growth phase and stored at −80 °C. Cytochrome *c*₅₅₂ was isolated by washing *T. thermophilus* cells with a high salt concentration in Tris-HCl (pH 7.6) and further purified according to the methods described in ref 12. The *ba*₃-type cytochrome *c* oxidase was prepared according to a new protocol; 100 g of frozen cells was thawed in 500 mL of 100 mM Tris-HCl (pH 7.6) containing 200 mM KCl, and 800 mg of lysozyme was added. After a 60 min stirring period, the suspension was centrifuged. For the solubilization of the respiratory complexes, the pellet was resuspended in 500 mL of 100 mM Tris-HCl (pH 7.6), adjusted to 5% Triton X-100, stirred for 3 h, and centrifuged at 17700g (Beckman JA-10 rotor, 10 000 rpm) at 4 °C. The supernatant was diluted with 5 L of H₂O and chromatographed on a DEAE-Biogel Agarose column (Bio-Rad) in 0.1% Triton X-100 and 10 mM Tris-HCl (pH 7.6). Fractions containing the *ba*₃ oxidase were pooled, concentrated, and rechromatographed twice on Fractogel EMD TMAE-650 (S) (MERCK); the detergent 0.1% Triton X-100 was changed to 0.05% dodecyl β-D-maltoside. Fractions containing *ba*₃ oxidase were again collected, concentrated, and purified by gel filtration on

Superdex 200 (Pharmacia) in 50 mM Tris-HCl (pH 7.6) containing 0.1% dodecyl β-D-maltoside. The purified *ba*₃ oxidase was concentrated by ultrafiltration (Centricon 100000, Amicon), desalted by passing it through a Sephadex G-25 column, shock frozen in liquid nitrogen, and stored at −74 °C. Immediately before spectroscopic investigation, the sample was thawed and diluted to the required concentration in 100 mM Tris-HCl (pH 7.6) containing dodecyl β-D-maltoside. More details and a protein chemical characterization of the enzyme will be published with the X-ray data (T. Soulimane and G. Buse, unpublished results).

The concentrations of cyt *c*₅₅₂ and *ba*₃ were determined by using the following extinction coefficients: $\epsilon_{552,\text{red}} = 21.1 \text{ mM}^{-1} \text{ cm}^{-1}$ and $\epsilon_{416,\text{ox}} = 152 \text{ mM}^{-1} \text{ cm}^{-1}$, respectively.

Spectrophotometric and Polarographic Measurements. CO titrations were monitored by a double-beam spectrophotometer (Jasco V-570). The samples were contained in a 1 cm light path sealed cuvette, where the gas phase in the cuvette was reduced as much as possible.

The reduced minus oxidized spectrum of heme *b* was obtained as the difference between the spectrum of dithionite-reduced minus oxidized CN-*ba*₃. The spectrum of F was obtained by addition of 5 mM H₂O₂ to oxidized beef heart *aa*₃ according to Vygodina et al. (28), since this protocol was unsuccessful with *ba*₃.

Polarographic measurements were carried out using a magnetic bar-stirred cell containing a Clark-type O₂ electrode.

Time-Resolved Spectroscopy. Stopped-flow experiments were carried out with a Durrum-Gibson thermostated instrument equipped with a single-wavelength apparatus (DX.17MV, Applied Photophysics, Leatherhead, U.K.) or with a diode array (TN6500, Tracor Northern, Madison, WI). The single-wavelength stopped-flow instrument has a dead time of ≈1 ms and a light path of 1 cm and can work in a sequential mixing mode, allowing two sequential mixing events with a preset delay time in between. The diode array apparatus can acquire as a function of time up to 80 spectra of 1024 elements, with an acquisition time of 10 ms per spectrum, and has a 2 cm light path.

Data Analysis. Data analysis was performed with the software MATLAB (MathWorks). Spectral deconvolution was achieved starting from reference spectra by using the “left division” option, provided by MATLAB. Spectral analysis was performed by using the singular value decomposition (SVD) algorithm according to Henry and Hofrichter (29).

RESULTS

Electron Entry into *ba*₃ Oxidase. The kinetics of eT from reduced cyt *c*₅₅₂ to *ba*₃, previously inhibited by cyanide, was followed at 25 °C as a function of substrate concentration. As already reported (16), the formation of the cyanide complex starting from oxidized *ba*₃ demanded prolonged incubation with cyanide (several days at 45 °C) and resulted in a one-electron reduced enzyme, with cyanide bound to reduced cyt *a*₃ [already characterized by RR studies (16, 17)]. Upon mixing this cyanide-bound *ba*₃ with reduced cyt *c*₅₅₂, fast oxidation of cyt *c*₅₅₂ was observed at 418 nm as an absorbance decrease. The time course followed within the experimental error an exponential decay, and the resulting

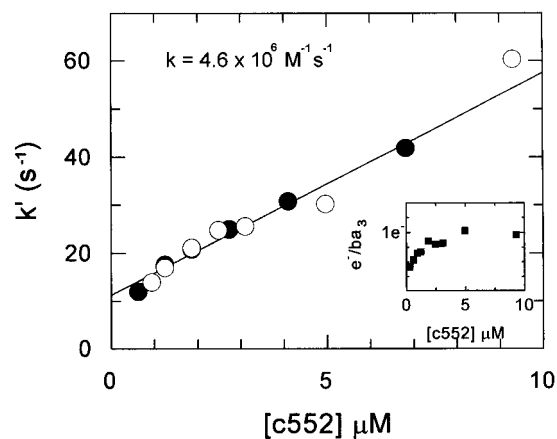


FIGURE 1: Electron transfer between cyt c_{552} and ba_3 . Rate constants relative to the exponential fit of cyt c_{552} oxidation, as monitored at 418 nm (isosbestic for cyt b reduction) after mixing at 25 °C cyanide-inhibited ba_3 (1 μ M) with reduced cyt c_{552} at different concentrations (from 0.6 to 18.6 μ M) in two different stopped-flow experiments: (●) 2 mM Tris (pH 7.6), 0.1% lauryl maltoside, and 50 mM NaCl and (○) 0.1 M Tris (pH 7.6) and 0.05% lauryl maltoside. From linear regression of the data, we obtained a bimolecular rate constant k of $4.6 \times 10^6 \text{ M}^{-1} \text{ s}^{-1}$. (Inset) Number of electrons entering into cyanide-inhibited ba_3 as a function of cyt c_{552} concentration.

rate constant was plotted as a function of cyt c_{552} concentration in Figure 1. Regression analysis of these data yields a bimolecular rate constant ($k = 4.6 \times 10^6 \text{ M}^{-1} \text{ s}^{-1}$) smaller than that typical for horse heart cyt c and beef heart aa_3 oxidase at a similar ionic strength and 8 °C [$k \approx 1 \times 10^8 \text{ M}^{-1} \text{ s}^{-1}$ (30)]; this difference is likely to be accounted for by an experimental temperature (25 °C) far from the physiological temperature for ba_3 (>70 °C, see below). Nevertheless, the relatively fast cyt c_{552} oxidation (despite the nonphysiological temperature) further supports the proposal that cyt c_{552} is the substrate for ba_3 oxidase (12). We notice that the regression line in Figure 1 does not go through the origin of Y-axis. For a simple binding process, this would indicate a significant dissociation rate constant of the complex, whereas in this case, since the reaction is much more complicated, an unequivocal interpretation for the intercept cannot be given. Therefore, from the data in Figure 1, we extracted only information on the apparent bimolecular rate constant of the forward reaction.

A partially unexpected result came from the analysis of the amplitude of the reaction. The number of electrons transferred per enzymatic functional unit (inset of Figure 1) is, under all conditions, considerably less than two (a value expected, in analogy to beef heart oxidase, if complete reduction of Cu_A and cyt b occurred). Since the redox potentials of cyt c_{552} [230 mV (31)] and Cu_A of uncomplexed ba_3 [250 mV, as determined at pH 8 in the isolated Cu_A domain (32)] are quite "normal", in cyanide-bound ba_3 the redox potential of the Cu_A –cyt b pair may be drastically lowered. This hypothesis, though far from being proven, is consistent with the finding that in these experiments cyt b is only partially reduced (<75%), as inferred from the absorption changes recorded at 410 nm, a wavelength isosbestic for cyt c_{552} (not shown).

To explore the effect of high temperatures on the intermolecular eT rate between cyt c_{552} and ba_3 , the experiment just described was carried out at different temperatures

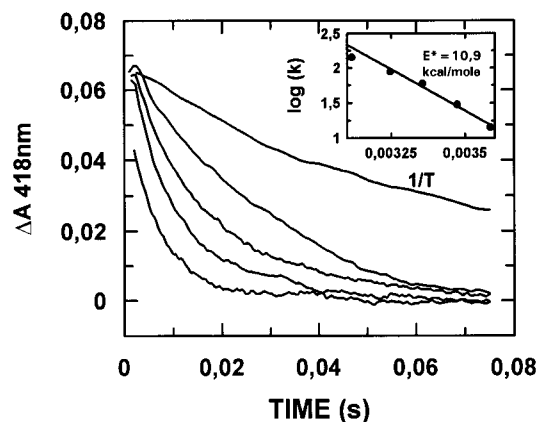


FIGURE 2: Effect of temperature on electron transfer between cyt c_{552} and ba_3 . Time courses observed at 418 nm after mixing reduced cyt c_{552} (11 μ M) with ba_3 (2 μ M) at increasing temperatures ($T = 6, 15, 25, 35$, and 48 °C; traces from the top right to bottom left). (Inset) Arrhenius plot of the oxidation of cyt c_{552} , yielding an activation energy E^* of $10.9 \pm 0.9 \text{ kcal mol}^{-1}$.

up to 50 °C (Figure 2), which (as far as we know) has not been attempted before. As expected, the rate of intermolecular eT constantly increased at higher temperatures, yielding an activation energy E^* of $10.9 \pm 0.9 \text{ kcal mol}^{-1}$. This result is a clear indication that the cyt c_{552} binding site of ba_3 is structurally highly thermostable and evolutionary designed to allow eT even at high temperatures. If linearity of the Arrhenius plot shown in Figure 2 is assumed, the calculated second-order rate constant (k) for eT between cyt c_{552} and ba_3 oxidase at 70 °C would be $5 \times 10^7 \text{ M}^{-1} \text{ s}^{-1}$.

Interestingly, we found that ruthenium hexamine, an efficient positively charged electron donor for beef heart oxidase, is in contrast a poor electron donor for ba_3 oxidase. At a concentration of 500 μ M, ruthenium hexamine reduces cyt b in the cyanide complex only at a k' of 0.9 s^{-1} at 20 °C (not shown). On the contrary, TMPD at the same temperature has an apparent bimolecular rate constant ($k = 2.9 \times 10^3 \text{ M}^{-1} \text{ s}^{-1}$, not shown) essentially identical to that reported for beef heart oxidase. When these results are taken into account together with the peculiar charge distribution found on the surface of cyt c_{552} (13), it is not totally immaterial to expect some relevant differences in the charge distribution within the cyt c binding site of ba_3 .

Effect of Temperature and Ionic Strength on the Activity of ba_3 . We examined the cyt c_{552} oxidase activity of ba_3 in the temperature range of 7–65 °C, by measuring the time course of oxidation of cyt c_{552} . The results indicate that up to ≈ 60 °C the enzymatic activity is enhanced, with an activation energy E^* of $11 \pm 1.4 \text{ kcal mol}^{-1}$, showing that at higher temperatures ba_3 is not only reduced by cyt c_{552} but also fully competent in catalysis (not shown). In these experiments, ba_3 proved to be highly thermostable, showing identical activity before and after incubation for 2 h at 50 °C.

More surprising is the effect of ionic strength on the activity of ba_3 oxidase. In these experiments, the ionic strength was increased from very low to 152 mM by addition of KCl (or MgSO_4 , not shown) and the activity of 1 nM ba_3 measured in the presence of 1.2 μ M cyt c_{552}^{2+} . As shown in Figure 3, the activity drops upon increasing the ionic strength, regardless of the temperature (25 or 50 °C). The very same ionic strength dependence at 25 °C was also observed at

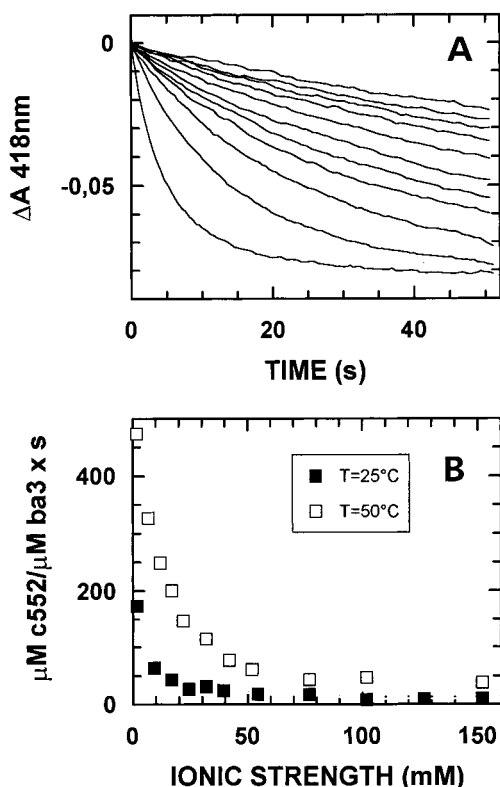


FIGURE 3: Effect of ionic strength on the activity of *ba*₃. (A) Time courses of oxidation of cyt *c*₅₅₂ (1.2 μ M) by *ba*₃ (1 nM) at 25 °C, as monitored at 418 nm. The buffer was 2 mM Tris (pH 7.6) and 0.1% lauryl maltoside and the ionic strength adjusted (between 1.8 and 152 mM) by addition of KCl. (B) Effect of ionic strength on *ba*₃ oxidase activity (at 25 and 50 °C), as measured from the initial rate of cyt *c*₅₅₂ oxidation. Interestingly, the maximal activity is observed at the lowest ionic strength, where activity of beef heart or *P. denitrificans aa*₃ is extremely low (25, 26).

higher concentrations of cyt *c*₅₅₂ and *ba*₃ (11.2 μ M and 250 nM, respectively, not shown); in this case, as expected, we measured higher turnover numbers. This effect of ionic strength is remarkable, being different from what is known for the interaction between horse heart cyt *c* and beef heart cytochrome oxidase (25) or *P. denitrificans aa*₃ (26), which are almost inactive at very low ionic strengths due to formation of a stable electrostatic complex (27). Thus, by analogy, we may presume that in the case of the *ba*₃ enzyme, a stable electrostatic complex with cyt *c*₅₅₂ is not formed even at low ionic strengths, a result in line with some peculiarities in the interaction between *ba*₃ and cyt *c*₅₅₂.

Oxygen Reaction. Contrary to all other heme–copper oxidases, whose O₂ reaction is very fast and thus investigated with the flow-flash technique (33), the O₂ reaction of *ba*₃ was found to be remarkably slow, allowing its kinetic investigation by the stopped-flow method (Figure 4). When *ba*₃ oxidase, previously degassed and reduced by ascorbate and ruthenium hexamine, is mixed at 4.5 °C with air-equilibrated buffer, three kinetic phases were observed: (i) a fast approach to steady state (representing the O₂ reaction), (ii) the steady-state phase, and (iii) the re-reduction of *ba*₃ by excess reductants when O₂ is used up. Under our experimental conditions (low temperature and ruthenium hexamine as the electron donor), the activity of *ba*₃ is remarkably slow and consistently the steady-state phase is very long (minutes). We focused on the fastest phase by collecting optical spectra between 1 and 50 ms from 390 to

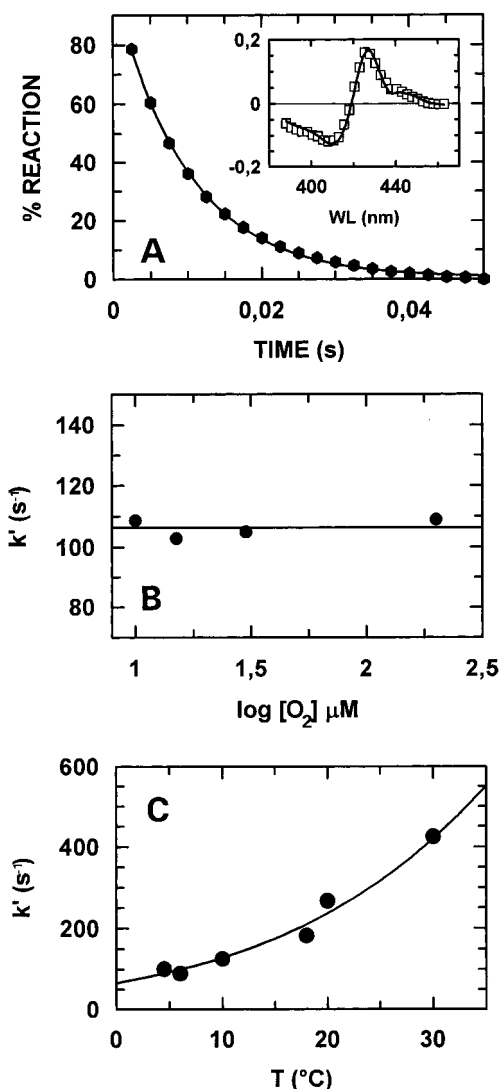


FIGURE 4: O₂ reaction. (A) Exponential fit of the first V column of the SVD output of absorption changes collected (from 390 to 465 nm) on mixing *ba*₃ (5 μ M), previously degassed and reduced by 5 mM ascorbate and 500 μ M ruthenium hexamine, with air-equilibrated buffer at 4.5 °C; $k' = 101 \text{ s}^{-1}$. (Inset) Kinetic difference spectrum observed during the O₂ reaction (\square) and the fit (solid line) obtained by summing the reduced minus oxidized optical contribution of cyt *b* (1.8 μ M) and the F minus oxidized spectrum (1.4 μ M). (B) Rate constant observed at 428 nm at different O₂ concentrations (experimental conditions as described for panel A). (C) Effect of temperature on the O₂ reaction as monitored at 433 nm and 10 μ M O₂. $E^* = 10.1 \pm 0.9 \text{ kcal mol}^{-1}$.

465 nm (with a 2.5 nm interval). SVD analysis of these data clearly shows that only one optical transition is revealed with an exponential time course proceeding at $k' = 100 \text{ s}^{-1}$. The kinetic difference spectrum is consistent with oxidation of (1.8 μ M) cyt *b* synchronous to the decay of (1.4 μ M) F intermediate to oxidized cyt *a*₃–Cu_B (Figure 4A); the data were fitted using the reduced minus oxidized difference spectrum of cyt *b* of *ba*₃ and the F minus oxidized difference spectrum of beef heart oxidase. Due to the very similar optical features of F and P in the Soret region (34), we cannot assess a priori which of the two intermediates is responsible for observed absorption changes. Nevertheless, by analogy with mitochondrial oxidase where the decay of F is the slowest event in the O₂ reaction (proceeding at a k' of 700–1,000 s^{-1} ; see refs 35–37 for reviews), it is likely that also in the case of *ba*₃ this is the slowest process.

The kinetics of this process was found to be independent of O_2 concentration from 5 to 190 μM (Figure 4B), indicating that the eT process monitored is after (and not rate-limited by) the much faster combination of O_2 to the reduced cyt a_3 - Cu_B site. The relatively slow rate observed [$k' = 100$ s^{-1} compared with $k' = 700$ – 1.000 s^{-1} for beef heart aa_3 (35–37)] is likely to be due to an experimental temperature (4.5 $^{\circ}C$) very far from the physiological temperature for *T. thermophilus* (>70 $^{\circ}C$). To explore this hypothesis, we followed the O_2 reaction at higher temperatures and interestingly observed that at 30 $^{\circ}C$ the reaction is already close to the time resolution limit of the stopped-flow apparatus ($k' \approx 400$ s^{-1} , Figure 4C); from the temperature dependence in the range of 5–30 $^{\circ}C$, we estimated an activation energy E^* of 10.1 ± 0.9 kcal mol^{-1} .

Effect of Temperature on CO Binding and Dissociation. The overall affinity of reduced ba_3 for CO was estimated by performing at 20 $^{\circ}C$ a static spectrophotometric titration in the Soret and visible regions. SVD analysis of the collected spectra reveals only one optical transition corresponding to CO binding to cyt a_3^{2+} with an overall affinity constant K_{eq} of 1.1×10^5 M^{-1} (Figure 5A). It is interesting to notice that, despite the measured affinity, at room temperature and under 1 atm of CO about 30% of the ba_3 seems to be unligated, as inferred by MCD (18). On the other hand, we also reproduced such observation by mixing at 20 $^{\circ}C$ in the diode array stopped-flow apparatus dithionite-reduced ba_3 pre-equilibrated with 1 mM CO, with a solution containing 1 mM NO; under these conditions, the spectrum collected 10 ms after mixing (when photodissociation produced by the incident light beam is negligible) shows already the optical features of NO bound to about 30% of ba_3 (not shown). This confirms that there is a significant fraction of ba_3 that is unligated and, thus, freely accessible to NO.

The effect of temperature on the kinetics of CO binding to ba_3 was investigated by anaerobically mixing in the stopped-flow apparatus dithionite-reduced ba_3 with 100 μM CO in the temperature range of 5–70 $^{\circ}C$ and monitoring the absorption changes at 444 nm. At each temperature, the time course of CO binding is monophasic and the corresponding apparent rate constant was obtained by fitting the traces to simple exponential decays. The raw data clearly show (Figure 5B) that on increasing the temperature (i) CO combination is faster and (ii) above 25 $^{\circ}C$ the amount of CO complex formed constantly decreases. This is a strong indication that increasing temperature lowers the overall binding constant for CO binding to reduced ba_3 (K_{eq}). The equilibrium constant (K_{eq}) at the different temperatures was estimated from the fraction of CO- ba_3 formed at $t \rightarrow \infty$, neglecting the amount of bound CO with respect to total CO; from the temperature dependence of K_{eq} , we estimated a ΔH of -12.7 ± 0.6 kcal mol^{-1} (inset of Figure 5B). Taking into account that under all conditions the apparent rate constant $k' = k_{on}[CO] + k_{off}$ (where k_{on} and k_{off} are the combination and dissociation rate constants for CO, respectively) and that $K_{eq} = k_{on}/k_{off}$, we calculated the contribution of k_{off} from the experimentally measured apparent rate constant at the different temperatures (Figure 5B). Notice that according to this analysis, k_{off} is expected to have a strong temperature dependence ($E^* = 19.8 \pm 1.2$ kcal mol^{-1}).

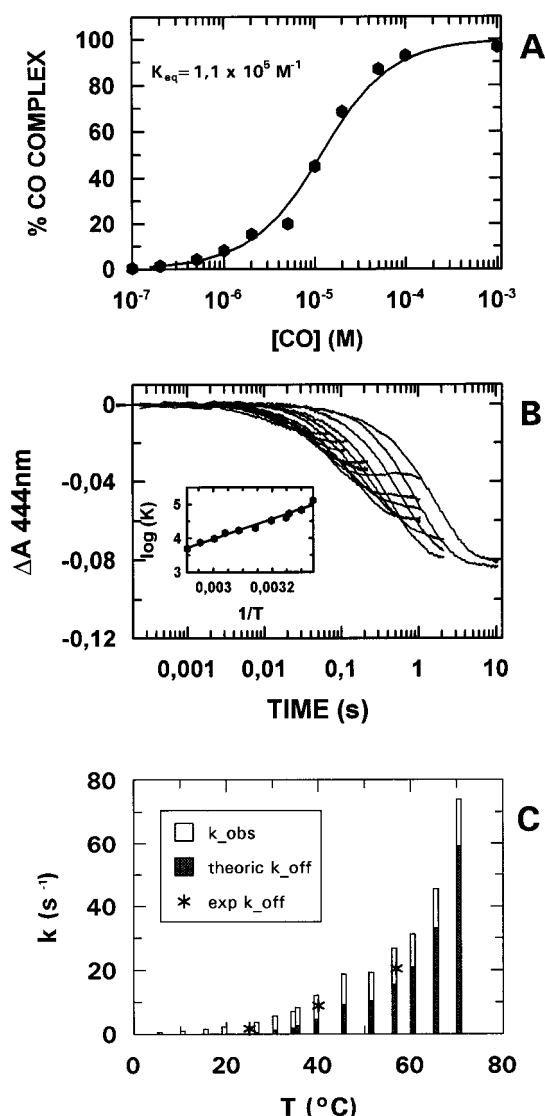


FIGURE 5: CO binding and dissociation. (A) Titration profile obtained by SVD analysis of the spectra obtained by incubating dithionite-reduced ba_3 (3.9 μM) with CO (from 0.1 to 100 μM) at 20 $^{\circ}C$. The best fit yields an equilibrium constant K_{eq} of 1.1×10^5 M^{-1} . (B) Time courses collected at 444 nm after mixing dithionite-reduced ba_3 with 100 μM CO at temperatures from 5 to 70 $^{\circ}C$ (traces from right to left). Time courses were fitted to single-exponential decays, and from the fraction of CO complex formed at $t \rightarrow \infty$, K_{eq} was estimated at the different temperatures. (Inset) The van't Hoff plot of estimated K_{eq} values yields a ΔH of -12.7 ± 0.6 kcal mol^{-1} . (C) Temperature dependence of the observed rate constant. The contribution of k_{off} to the observed rate constant at each temperature was calculated from the value of K_{eq} estimated from panel B at the same temperature. Asterisks denote experimental k_{off} values measured by mixing with 1 mM NO a solution containing ba_3 , prerduced with ascorbate (10 mM) and TMPD (100 μM) and incubated with 100 μM CO.

This analysis estimates an overall equilibrium constant for CO binding to ba_3 at 20 $^{\circ}C$ ($K_{eq} = 1.3 \times 10^5$ M^{-1}) that is in very good agreement with that experimentally measured by static titration ($K_{eq} = 1.1 \times 10^5$ M^{-1}). This value is however ≈ 40 -fold smaller than that reported for beef heart aa_3 [$K_{eq} = 3.9 \times 10^6$ M^{-1} (33)]. On the other hand, $K_{eq} = K_1 K_2$, where K_1 is the affinity constant of CO for Cu_B^{+} and K_2 is the equilibrium constant for CO transfer to cyt a_3^{2+} (see Scheme 1). Since K_1 was reported to be for ba_3 at least 100-fold larger than the corresponding value for beef heart oxidase (see Table 1), we expect K_2 for ba_3 to be at least

Table 1: Kinetic and Thermodynamic Parameters for CO Binding to *ba*₃ of *T. thermophilus* and Beef Heart *aa*₃ According to Scheme 1 in the Text^a

	k_F	k_R (s ⁻¹)	$K =$ k_F/k_R	$K_{eq} =$ $K_{CuB}K_{a_3}$ (M ⁻¹)
bovine				
Cu _B	6.1×10^7 M ⁻¹ s ⁻¹	7×10^5	87 M ⁻¹	3.9×10^6
<i>a</i> ₃	1030 s ⁻¹	0.023	4.5×10^4	
<i>T. thermophilus</i>				
Cu _B	?	?	$> 10^4$ M ⁻¹	1.1×10^5
<i>a</i> ₃	8 s ⁻¹	0.8	10	

^a Data from this work are in bold; all other data are from ref 23.

4000-fold smaller than for beef heart oxidase. To test this expectation, we measured the thermal dissociation of CO from cyt *a*₃²⁺ of *ba*₃ by displacing CO from reduced *ba*₃ with NO (33). Thus, *ba*₃ reduced with ascorbate (10 mM) and TMPD (100 μM), and preincubated with 100 μM CO, was anaerobically mixed in the single-wavelength stopped-flow apparatus with 1 mM NO at 20 °C. In these experiments, the diode array stopped-flow apparatus was not used, since the intense white light emitted by this instrument photodissociates CO from cyt *a*₃²⁺ with an apparent rate constant (10 s⁻¹) that is much higher than the intrinsic dissociation rate constant. The absorbance decrease observed at 430 nm in the displacement experiment is consistent with that for the expected replacement of CO by NO (not shown). Although the analysis was complicated by an unfavorable signal-to-noise ratio and by a partially biphasic behavior, most of the reaction proceeded at a rate constant ($k_{off} = 0.8$ s⁻¹) that is much larger than that of beef heart *aa*₃ at the same temperature [$k_{off} = 0.023$ s⁻¹ (33)]. It is interesting to notice that both the high experimentally measured k_{off} (0.8 s⁻¹) and the determined K_{eq} (1.1×10^5 M⁻¹) nicely meet the previously determined (23) kinetic and thermodynamic parameters for CO reaction with *ba*₃ (see Table 1). We therefore believe that in the *ba*₃ oxidase at 20 °C, the high affinity reported for CO binding to Cu_B⁺ ($K_1 > 10^4$ M⁻¹) is compensated by a small equilibrium constant for CO transfer to cyt *a*₃²⁺ ($K_2 = 10$) to yield an overall affinity about 40-fold smaller than that reported for beef heart cyt oxidase.

The kinetics of CO dissociation from reduced *ba*₃ was investigated in the temperature range of 6–55 °C. The observed dissociation rate constant is strongly dependent on temperature, and this finding explains the large drop in affinity at higher temperatures. In Figure 5C, we compare the dissociation rate constants experimentally determined at three temperatures (25, 40, and 55 °C) with the values calculated from the fraction of the CO–*ba*₃ complex formed at equilibrium. The agreement among these data is a further indication of the validity of the analysis described above.

On the basis of these results, it is likely that the structure of the cyt *a*₃–Cu_B binuclear site of *ba*₃ oxidase displays peculiar features, as suggested also by the following results on the onset of inhibition by cyanide.

Onset of Inhibition by Cyanide. We measured polarographically the time required after addition of cyanide to completely inhibit the catalytic O₂ consumption of *ba*₃ oxidase sustained by cyt *c*₅₅₂ in the presence of excess ascorbate and TMPD; in parallel experiments, we tested the effect of cyanide on beef heart oxidase using horse heart

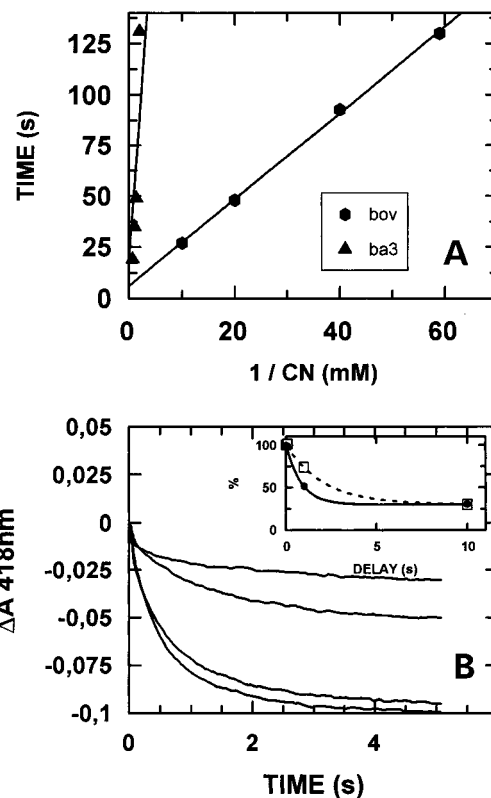


FIGURE 6: Onset of cyanide inhibition. (A) Time required for complete inhibition of *ba*₃ and bovine oxidase at increasing concentrations of CN⁻, as measured polarographically at room temperature. The enzyme concentration was 200 nM. O₂ consumption was sustained with 10 mM ascorbate, 1 mM TMPD, and either 6 μM cyt *c*₅₅₂ (for the *ba*₃ oxidase) or 0.6 μM horse heart cyt *c* (for the bovine enzyme). (B) Oxidation of reduced cyt *c*₅₅₂ measured at 418 nm at different delay times (from 10 ms to 10 s, traces from the bottom to the top) in the following sequential stopped-flow experiment: *ba*₃ oxidase (0.4 μM) was mixed at 55 °C with 2.5 μM cyt *c*₅₅₂²⁺ and 4 mM NaCN, and after a preset delay, this mixture was mixed with 2.5 μM cyt *c*₅₅₂²⁺. (Inset) Cyt *c*₅₅₂²⁺ oxidized after the second mixing as a function of the delay time at 20 °C (□) and 55 °C (●).

cyt *c* instead of cyt *c*₅₅₂. Conditions were set to achieve identical activity for both enzymes (≈ 50 μM O₂ μM oxidase⁻¹ s⁻¹). As shown in Figure 6A, *ba*₃ is much less sensitive to cyanide (30-fold) than beef heart oxidase, a result in line with the hypothesis of significant structural differences of the binuclear site.

At high cyanide concentrations (1–3 mM), we carried out a rapid mixing experiment making use of the sequential mixing stopped-flow instrument, following the experimental design used by Wilson et al. (38) for beef heart oxidase. Oxidized *ba*₃, rapidly mixed with reduced cyt *c*₅₅₂ and (4 mM) cyanide, is mixed with a second solution of reduced cyt *c*₅₅₂ after a preset delay (from 10 ms to 10 s). After the first mixing, cyt *c*₅₅₂ injects electrons into *ba*₃, triggering fast cyanide binding; this mixture is aged for a preset period of time (which allows progressive binding of cyanide) and then probed for the residual activity, by mixing with an additional aliquot of reduced cyt *c*₅₅₂. In such experiments, increasing the delay time results in a larger fraction of inhibited enzyme and consequently less cyt *c*₅₅₂ oxidized in the second mixing. Figure 6B shows the time courses observed at 55 °C by varying the delay time from 10 ms to 10 s. When the amount of cyt *c*₅₅₂ oxidized in the second mixing is plotted as a

function of the delay time (Figure 6B, inset), it is shown that within 10 s the inhibition is essentially complete, whereas cyanide at the same concentration takes several days to bind to oxidized *ba*₃.

DISCUSSION

The *ba*₃ oxidase from *T. thermophilus* is the protein of choice for studying the structure–function relationships of thermophilic heme–copper oxidases, for a number of reasons. The purified enzyme and its physiological substrate, cyt *c*₅₅₂, are highly thermostable, allowing kinetic investigations at temperatures close to the physiological temperature (>50 °C), which is an important task if we want to understand respiration and adaptation in thermophilic microorganisms. Moreover, structural investigation of *ba*₃ is at an advanced stage (11), and the three-dimensional structure of cyt *c*₅₅₂ is available (13), revealing interesting peculiar features; in conjunction with the availability of molecular genetic approaches (2), this seems to be an excellent system to investigate.

In this paper, we have studied in some detail the effect of temperature on the kinetics of eT and ligand binding of *ba*₃ oxidase, employing stopped-flow spectrophotometry. By and large, we found several peculiarities in the room-temperature reactions of *ba*₃ with cyt *c*₅₅₂, O₂, CO, and cyanide, which however make sense when the experimental temperature approaches the physiological range for this thermophilic enzyme (>70 °C). Thus, some of the kinetic parameters of *ba*₃ are unusually slow at mesophilic temperatures, whereas canonical kinetic behavior is restored at higher, more physiological temperatures. We believe that this result may provide a clue to understanding enzymatic thermophilicity, i.e., the property of thermophilic oxidases to be sufficiently active only at high temperatures (39).

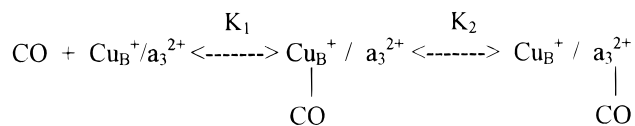
In this context, our results from the reaction of *ba*₃ oxidase with O₂ are particularly significant. With the other heme–copper oxidases, this reaction is usually too fast to be followed by stopped-flow methods (see refs 35–37 for reviews) and kinetic information was obtained by the flow-flash approach (33). According to a simplified consensus scheme (35), O₂ binding to the reduced cyt *a*₃–Cu_B site yields initially compound A, which decays to P (for peroxy) by two-electron delivery to bound O₂ and then to F (for ferryl) upon intramolecular donation of a third electron (35); the slowest step in the O₂ reaction is the transfer of the fourth electron at a *k'* of 700–1000 s^{−1} (at 20 °C), which yields the fully oxidized enzyme (O). We have shown above that the latter process can be easily observed by stopped-flow methods when mixing O₂ with reduced *ba*₃ oxidase, the reaction proceeding at a *k'* of ≈100 s^{−1} at 4.5 °C, independent of O₂ concentration from 10 to 190 μM (Figure 4). Analysis of the corresponding optical density changes (inset of Figure 4A) suggests that oxidation of cyt *b* is synchronous to the decay of the F intermediate. In view of the complexity of the overall scheme outlined above (35), we cannot rule out the possibility that the P intermediate is contributing to the observed absorption changes, given the similarity in the optical spectra of P and F in the Soret region (34); nevertheless, by analogy with the information already available in detail for beef heart oxidase (35–37), we assign the observed kinetic process at 100 s^{−1} to the decay of the

F intermediate. Since in beef heart oxidase the F → O transition was postulated to be coupled to proton pumping (35), a pH dependence of the kinetics of this process might be expected also for *ba*₃ oxidase, which was very recently proposed to be a proton pump (40). Interestingly, the rate of this process is strongly temperature-dependent (*E** = 10.1 ± 0.9 kcal mol^{−1}); at 40 °C, the reaction is already too fast to be followed by stopped-flow methods, and at 70 °C, the oxidation of cyt *b* is calculated to proceed at a *k'* of 3 × 10³ s^{−1}, consistent with high turnover. Thus, we have evidence that for this thermophilic enzyme, the last step in the overall O₂ reduction is characterized by a high activation barrier, whereby intramolecular eT to the last O₂ intermediate occurs with physiologically compatible kinetics only at high temperatures. In the absence of a three-dimensional structure of *ba*₃, we notice that thermophilic enzymes are generally characterized by enhanced rigidity of the protein matrix and tight packing of internal side chains, often associated with the absence of cavities and of internal water molecules (41). These structural features, besides accounting for thermostability, may be responsible for increased activation barriers (see ref 39 for a discussion). The finding that the slowest step in the O₂ reaction, i.e., the decay from F to O by intramolecular eT, is unusually slow is compatible with the expected decrease in flexibility and dynamics of these thermophilic enzymes.

The peculiar features of the three-dimensional structure of cyt *c*₅₅₂ (13) are (i) a C-terminal segment which wraps around the protein, (ii) an extended β-sheet shielding one edge of the heme, (iii) the lack of internal water molecules, and (iv) a peculiar dipole moment and a unique surface charge distribution. As discussed by Than et al. (13), some of these features are probably responsible for the high thermodynamic stability of this protein and the specificity in the reaction with *ba*₃ oxidase. Several lines of evidence indicating substantial peculiarities of the substrate binding site of *ba*₃ are now briefly discussed. The kinetics of reduction of *ba*₃ by ruthenium hexamine, which is an efficient reductant for beef heart oxidase [*k* = 1 × 10⁵ M^{−1} s^{−1} (42) to 2 × 10⁶ M^{−1} s^{−1}, depending on ionic strength], is slow; at 500 μM ruthenium hexamine, reduction of cyt *b* proceeds only at a *k'* of 0.9 s^{−1} compared with a *k'* of 250 s^{−1} observed for beef heart *aa*₃ at a similar ionic strength (not shown). This finding suggests some structural differences in the Cu_A domain on subunit II, at least in terms of surface charge distribution. The water soluble recombinant Cu_A domain of *ba*₃ was postulated to form an electrostatic complex with horse heart cyt *c* at low ionic strengths, as inferred from the perturbation of the absorption spectrum of cyt *c* when added to the isolated domain (32). The significance of this observation is however doubtful, given that the physiological electron donor to *ba*₃ is cyt *c*₅₅₂, as confirmed by the fast intermolecular eT measured in the present study (*k* = 4.6 × 10⁶ M^{−1} s^{−1} at 25 °C, Figure 1). In addition, we have shown that, regardless of temperature (25 or 50 °C), *ba*₃ displays maximal cyt *c*₅₅₂ oxidase activity at low ionic strengths (<10 mM, Figure 3), contrary to the case of cyt *c* oxidation by beef heart and *P. denitrificans aa*₃, which is very slow due to formation of the so-called high-affinity electrostatic complex (27). Our data in Figure 3 are peculiar and unique insofar as they show no evidence for a tight electrostatic complex between *ba*₃ and cyt *c*₅₅₂ at low ionic strengths,

contrary to what was observed with horse heart cyt *c*, which forms such a complex with both the mitochondrial (27) and thermophilic oxidases (32). Since the stability of this complex is due to charge complementarity and a favorable dipole moment, it is not surprising that no complex is formed between *ba*₃ and cyt *c*₅₅₂. We also notice that the calculated isoelectric point of *ba*₃ subunit II (*pI* = 6.4) is higher than that of the bovine (*pI* = 4.6) and *P. denitrificans* (*pI* = 4.7) enzymes, and particularly that two acidic residues involved in the binding of cyt *c* with *P. denitrificans* oxidase [i.e., Asp135 and Asp159 (26)] are absent in *ba*₃. Therefore, our kinetic data in Figure 3 are fully compatible with available structural information on *ba*₃ and its physiological substrate, and also suggest that "presentation" of cyt *c*₅₅₂ to the Cu_A site may occur via the same interface identified in the mammalian counterpart.

Peculiar structural features of the cyt *a*₃–Cu_B site of *ba*₃ oxidase were inferred from data obtained with different spectroscopic techniques, both static and combined with flash photolysis [FT-IR (15), RR and EPR (16, 17), and CD and MCD (18)]. Further evidence consistent with this information has emerged from our data on the onset of inhibition by cyanide under turnover conditions and particularly from the reaction of the reduced enzyme with CO. CO binding to reduced heme–copper oxidases, studied in great detail with the beef heart enzyme (23), is now known to occur in two steps according to Scheme 1:



CO binds first to Cu_B⁺ in a bimolecular low-affinity reaction and then is transferred intramolecularly to cyt *a*₃²⁺. Therefore, binding of CO to cyt *a*₃²⁺ may be described by two coupled equilibria, with an overall affinity constant (*K*_{eq}) given by the product of the two microscopic equilibrium constants (*K*₁ and *K*₂ in Scheme 1). Prior studies (15, 18) revealed that CO binding to *ba*₃ oxidase is peculiar because, contrary to the case of beef heart *aa*₃, Cu_B⁺ has a relatively high affinity for CO (*K*₁ > 10⁴ M^{−1}; see Table 1), whereas the transfer of the ligand to cyt *a*₃²⁺ is characterized by a small forward rate constant (*k*_F = 8 s^{−1}; see Table 1). This work was carried out either at cryogenic or at room temperatures and never addressed the determination of the thermal dissociation rate constant of CO from cyt *a*₃²⁺. We therefore extended the determination by (i) performing a static CO titration of reduced *ba*₃, (ii) following the combination of CO with reduced *ba*₃ over the temperature range of 5–70 °C, and (iii) measuring over the same temperature range the dissociation of CO from cyt *a*₃²⁺ by the classical ligand displacement method, making use of nitric oxide (33). An original result emerging from our study is that at 20 °C the overall affinity for CO of reduced *ba*₃ is ≈40-fold smaller than that of beef heart *aa*₃, despite the much larger affinity for Cu_B⁺ seen with the thermophilic enzyme (see Table 1). With reference to Scheme 1, this is due to a ligand transfer to cyt *a*₃²⁺, which in the *ba*₃ oxidase is thermodynamically less favorable. Such a phenomenon, previously postulated (18), has been quantitated by directly measuring the dissociation rate constant of CO from reduced *ba*₃ (*k*_{−2} = 0.8

s^{−1} at 20 °C), 30-fold greater than that of beef heart *aa*₃ [*k*_{−2} = 0.023 s^{−1} (33)]. This result allows the calculation of the equilibrium constant for intramolecular CO transfer to cyt *a*₃²⁺ which in *ba*₃ is too small (*K*₂ ≈ 10) to compensate for the higher affinity for Cu_B⁺ (*K*₁ > 10⁴ M^{−1}). The overall affinity constant measured by static titration of *ba*₃ (*K*_{eq} = 1.1 × 10⁵ M^{−1}, Figure 5A) appears to be inconsistent with the finding that reduced *ba*₃ incubated at room temperature under 1 atm of CO still contains ≈30% of cyt *a*₃²⁺ unligated, an observation already documented (18) and confirmed in the present study. A possible explanation for this inconsistency, based on the presence of a conformer unable to bind CO, is supported by detection of two conformers of *ba*₃ by Mössbauer, RR, and FT-IR spectroscopy (1, 15, 17). As an alternative, Goldbeck et al. (18) suggested that assuming a stoichiometry of one CO per site, cyt *a*₃²⁺ will never be 100% saturated with CO because of the partition with the nearby Cu_B⁺. Our data in Table 1 indicate that this fraction would be ≈10%, which may not be inconsistent with such a hypothesis.

This analysis of CO binding to reduced *ba*₃ leads to a novel hypothesis accounting for O₂ binding to thermophilic oxidases, with relevance for evolution and survival at high temperatures. It is now widely accepted that Cu_B⁺ may be viewed as the "gate" for binding of CO and O₂ to all heme–copper oxidases. In this context, the unusually high affinity of Cu_B⁺ for CO seen with *ba*₃, if extended to O₂, may have physiological relevance for thermophilic oxidases. The *ba*₃ oxidase is evolutionarily selected to work under environmental conditions with low O₂ tension, given the reduced gas solubility at high temperature and the microaerobic conditions in which this enzyme is preferentially expressed. Therefore, thanks to its higher affinity, Cu_B⁺ may be envisaged to act under physiological conditions as a more efficient "trap" for O₂, which is present at low concentrations in the bulk. The significance of this hypothesis would be reinforced if the affinity of Cu_B⁺ for O₂ was not significantly reduced at high temperatures. In the case of CO, the overall affinity of the thermophilic enzyme decreases from 5 to 70 °C (Figure 5B), but such an effect is predominantly due to a large increase of the rate constant for dissociation from cyt *a*₃²⁺ (Figure 5C). Since we expect that the O₂ dissociation rate constant will be effectively very small because of fast eT to bound O₂ [which traps the ligand at the binuclear center (43)], the postulated higher affinity of O₂ for Cu_B⁺ may effectively increase the likelihood of efficient O₂ binding under physiological conditions, with obvious advantages for survival at high temperatures. Scrolling the data presented by Woodruff (23), we notice that the two alternative oxidases of *T. thermophilus* (*caa*₃ and *ba*₃) are both characterized by CO affinity for Cu_B⁺ in the range of 10³–10⁴ M^{−1}, in contrast with the lower affinity characteristic of mesophilic oxidases (*K*_{eq} ≈ 10–100 M^{−1}). This consideration seems to confer generality to the hypothesis discussed above, though living unsettled the structural basis for the enhanced affinity of gaseous ligands for Cu_B⁺, an interesting problem which we are hopeful will be understood when the structure is solved.

In conclusion, in this paper we show that the *ba*₃ oxidase of *T. thermophilus* is characterized by several peculiar features in the kinetics of eT and ligand binding, which likely emerged during evolution in response to adaptation to high temperatures. These peculiar kinetic properties should obvi-

ously reflect differences in the three-dimensional structure of the enzyme, and we believe that, once this structure will be available, correlation of functional and structural findings will provide some insight into the understanding of evolution and adaptation of thermophilic heme-copper oxidases.

REFERENCES

- Zimmermann, B. H., Nitsche, C. I., Fee, J. A., Rusnak, F., and Münck, E. (1988) *Proc. Natl. Acad. Sci. U.S.A.* 85, 5779–5783.
- Keightley, J. A., Zimmermann, B. H., Mather, M. W., Springer, P., Pastuszyn, A., Lawrence, D. M., and Fee, J. A. (1995) *J. Biol. Chem.* 270, 20345–20358.
- Castresana, J., Lübken, M., Saraste, M., and Higgins, D. G. (1994) *EMBO J.* 13, 2516–2525.
- Schäfer, G., Purschke, W., and Schmidt, C. L. (1996) *FEMS Microbiol. Rev.* 18, 173–188.
- Lübken, M., Kolmerer, B., and Saraste, M. (1992) *EMBO J.* 11, 805–812.
- Giuffrè, A., Antonini, G., Brunori, M., D'Itri, E., Malatesta, F., Nicoletti, F., Anemüller, S., Gleissner, M., and Schäfer, G. (1994) *J. Biol. Chem.* 269, 31006–31011.
- Gleissner, M., Kaiser, U., Antonopoulos, E., and Schäfer, G. (1997) *J. Biol. Chem.* 272, 8417–8426.
- Anemüller, S., Schmidt, C. L., Pacheco, I., Schäfer, G., and Teixeira, M. (1994) *FEMS Microbiol. Lett.* 117, 275–280.
- Purschke, W. G., Schmidt, C. L., Petersen, A., and Schäfer, G. (1997) *J. Bacteriol.* 179, 1344–1353.
- Giuffrè, A., Gomes, C. M., Antonini, G., D'Itri, E., Teixeira, M., and Brunori, M. (1997) *Eur. J. Biochem.* 250, 383–388.
- Soulimane, T., Gohlke, U., Huber, R., and Buse, G. (1995) *FEBS Lett.* 368, 132–134.
- Soulimane, T., von Walter, M., Hof, P., Than, M. E., Huber, R., and Buse, G. (1997) *Biochem. Biophys. Res. Commun.* 237, 572–576.
- Than, M. E., Hof, P., Huber, R., Bourenkov, G. P., Bartunik, H. D., Buse, G., and Soulimane, T. (1997) *J. Mol. Biol.* 271, 629–644.
- Hon-nami, K., and Oshima, T. (1979) *Biochemistry* 18, 5693–5697.
- Einarsdóttir, O., Killough, P. M., Fee, J. A., and Woodruff, W. H. (1989) *J. Biol. Chem.* 264, 2405–2408.
- Surerus, K. K., Oertling, W. A., Fan, C., Gurbiel, R. J., Einarsdóttir, O., Antholine, W. E., Dyer, R. B., Hoffman, B. M., Woodruff, W. H., and Fee, J. A. (1992) *Proc. Natl. Acad. Sci. U.S.A.* 89, 3195–3199.
- Oertling, W. A., Surerus, K. K., Einarsdóttir, O., Fee, J. A., Dyer, R. B., and Woodruff, W. H. (1994) *Biochemistry* 33, 3128–3141.
- Goldbeck, R. A., Einarsdóttir, O., Dawes, T. D., O'Connor, D. B., Surerus, K. K., Fee, J. A., and Kliger, D. S. (1992) *Biochemistry* 31, 9376–9387.
- Yoshikawa, S., Shinzawa-Itoh, K., Nakashima, R., Yaono, R., Yamashita, E., Inoue, N., Yao, M., Fei, M. J., Libeu, C. P., Mizushima, T., Yamaguchi, H., Tomizaki, T., and Tsukihara, T. (1998) *Science* 280, 1723–1729.
- Tsukihara, T., Aoyama, H., Yamashita, E., Tomizaki, T., Yamaguchi, H., Shinzawa-Itoh, K., Nakashima, R., Yaono, R., and Yoshikawa, S. (1996) *Science* 272, 1136–1144.
- Tsukihara, T., Aoyama, H., Yamashita, E., Tomizaki, T., Yamaguchi, H., Shinzawa-Itoh, K., Nakashima, R., Yaono, R., and Yoshikawa, S. (1995) *Science* 269, 1069–1074.
- Iwata, S., Ostermeier, C., Ludwig, B., and Michel, H. (1995) *Nature* 376, 660–669.
- Woodruff, W. H. (1993) *J. Bioenerg. Biomembr.* 25, 177–188.
- Einarsdóttir, O., Dyer, R. B., Lemon, D. D., Killough, P. M., Hubig, S. M., Atherton, S. J., López-Garriga, J. J., Palmer, G., and Woodruff, W. H. (1993) *Biochemistry* 32, 12013–12024.
- Bolli, R., Nalecz, K. A., and Azzi, A. (1985) *Biochimie* 67, 119–128.
- Witt, H., Malatesta, F., Nicoletti, F., Brunori, M., and Ludwig, B. (1998) *Eur. J. Biochem.* 251, 367–373.
- Michel, B., and Bosshard, H. R. (1984) *J. Biol. Chem.* 259, 10085–10091.
- Vygodina, T. V., Schmidmaier, K., and Konstantinov, A. A. (1993) *Biol. Membr.* 6, 883–906.
- Henry, E., and Hofrichter, J. (1992) *Methods Enzymol.* 210, 129–192.
- Antalis, T. M., and Palmer, G. (1982) *J. Biol. Chem.* 257, 6194–6206.
- Hon-nami, K., and Oshima, T. (1977) *J. Biochem. (Tokyo)* 82, 769–776.
- Slutter, C. E., Langen, R., Sanders, D., Lawrence, S. M., Wittung, P., Di Bilio, A. J., Hill, M. G., Fee, J. A., Richards, J. H., Winkler, J. R., and Malmström, B. G. (1996) *Inorg. Chim. Acta* 243, 141–145.
- Gibson, Q. H., and Greenwood, C. (1963) *Biochem. J.* 86, 541–555.
- Fabian, M., and Palmer, G. (1995) *Biochemistry* 34, 13802–13810.
- Babcock, G. T., and Wikström, M. (1992) *Nature* 356, 301–309.
- Malatesta, F., Antonini, G., Sarti, P., and Brunori, M. (1995) *Biophys. Chem.* 54, 1–33.
- Einarsdóttir, O. (1995) *Biochim. Biophys. Acta* 1229, 129–147.
- Wilson, M. T., Antonini, G., Malatesta, F., Sarti, P., and Brunori, M. (1994) *J. Biol. Chem.* 269, 24114–24119.
- Giuffrè, A., Watmough, N. J., Giannini, S., Brunori, M., Konings, W. N., and Greenwood, C. (1999) *Biophys. J.* (in press).
- Kannt, A., Soulimane, T., Buse, G., Becker, A., Bamberg, E., and Michel, H. (1998) *FEBS Lett.* 434, 17–22.
- Jaenicke, R. (1996) *FASEB J.* 10, 84–92.
- Scott, R. A., and Gray, H. B. (1980) *J. Am. Chem. Soc.* 102, 3219–3224.
- Verkhovsky, M. I., Morgan, J. E., Puustinen, A., and Wikström, M. (1996) *Nature* 380, 268–270.

BI9815389